

Long-term Stress Distribution Patterns Across the Ankle Joint in Soccer Players

A Computed Tomography Osteoabsorptiometry Study

Junki Shiota,* MD, Daisuke Momma,^{†‡} MD, PhD, Takayoshi Yamaguchi,[§] PhD, and Norimasa Iwasaki,* MD, PhD

Investigation performed at the Center for Sports Medicine, Hokkaido University Hospital, Sapporo, Japan

Background: The distribution pattern of subchondral bone density is considered to accurately reflect the stress distribution over a joint under long-term physiologic loading. The biomechanical characteristics of the surface of the ankle joint in soccer players can be determined by measuring this distribution pattern under long-term loading.

Purpose: To evaluate the distribution of subchondral bone density across the ankle joint in soccer players and to determine the effects of soccer activities, including kicking motion, on the ankle joint surface under long-term loading conditions by computed tomography (CT) osteoabsorptiometry (CTOAM).

Study Design: Cross-sectional study; Level of evidence, 3.

Methods: CT imaging data were obtained from both ankles of 10 soccer players (soccer group) and 10 nonathletic volunteers (control group). The distribution patterns of subchondral bone density across the articular surface of the ankle joints were assessed by CTOAM. Quantitative analysis was performed of the locations and percentages of high-density areas on the articular surface.

Results: Stress distribution patterns over the ankle joint differed between the soccer players and controls. In the soccer players, the high-density areas were found in the anterior part of the distal tibia and proximal talus as well as the distal fibula. The percentages of high-density areas were greater in the soccer players compared with controls ($P < .0001$).

Conclusion: Stress distribution over the articular surface of the ankle joint was affected by soccer activities. A high stress concentration was seen in soccer players in the anterior part of the tibia and talus and in the fibula; such excessive stress may lead to anterior impingement.

Keywords: soccer; ankle; CT osteoabsorptiometry; stress distribution

[‡]Address correspondence to Daisuke Momma, MD, PhD, Center for Sports Medicine, Hokkaido University Hospital, Kita 14, Nishi 5, Sapporo, Hokkaido 060-8638, Japan (email: d-momma@med.hokudai.ac.jp).

*Faculty of Medicine and Graduate School of Medicine, Department of Orthopaedic Surgery, Hokkaido University, Sapporo, Japan.

[†]Center for Sports Medicine, Hokkaido University Hospital, Sapporo, Japan.

[§]Hanaoka Seishu Memorial Hospital, Sapporo, Japan.

Final revision submitted April 26, 2020; accepted June 3, 2020.

The authors declared that there are no conflicts of interest in the authorship and publication of this contribution. AOSSM checks author disclosures against the Open Payments Database (OPD). AOSSM has not conducted an independent investigation on the OPD and disclaims any liability or responsibility relating thereto.

Ethical approval for this study was obtained from Hokkaido University Hospital (ref No. 017-0106).

The Orthopaedic Journal of Sports Medicine, 8(11), 2325967120963085

DOI: 10.1177/2325967120963085

© The Author(s) 2020

Soccer is among the most popular sports in the world, with more than 265 million young players,⁵ and participation has increased worldwide over the past decade. Soccer players frequently sustain severe injuries, such as fractures and ligament injuries, and the majority of them involve the lower extremities.^{1,10} The ankle is the most frequently injured site in the lower extremity of soccer players.²¹ The ankle is exposed to many different types of stresses, including repetitive motion, high-impact loading, axial compression, torsional forces, and distraction.² Combining these forces with varying degrees of varus and valgus and dorsiflexion predisposes the ankle to higher rates of ligament and bone injury during soccer activities.

Repetitive mechanical stress acting on the ankle during soccer activities is considered to be a cause of pathological conditions. To date, several biomechanical and cadaveric studies have examined ligament tension around the ankle during soccer activities.¹⁹ It is believed that soccer

activities probably alter the cumulative forces and stress distributions acting on the ankle. However, because of the difficulties^{6,8} in directly measuring these forces and stresses, the abnormal stress distributions across the ankle joint associated with soccer activities have not been confirmed. To develop treatment and prevention strategies for the pathological conditions mentioned above, it is necessary to elucidate the biomechanical characteristics of the ankle under the actual loading conditions of soccer activities.

The pattern of subchondral bone density reportedly reflects the distribution of cumulative stresses acting on a joint surface under actual loading conditions.¹⁷ Previous studies have shown that computed tomography (CT) osteoabsorptiometry (CTOAM) has potential for evaluating cumulative stress distribution patterns in elbow joints.^{14,16} The theoretical background of this method is that subchondral bone mineralization adapts functionally to repeated and long-term changes in joint loading. These studies found various stress distribution patterns in patients who were asymptomatic overhead throwers. Presumably, the change in subchondral bone density would be one way to indirectly assess alterations in stress distribution in the joints of asymptomatic soccer players and would reflect stress on the tissues.

We speculated that soccer activities would produce different patterns in the subchondral bone mineral density of the ankle in soccer players compared with nonathletic controls. Hence, using a modified CTOAM method, we analyzed stress distribution patterns and controls through the entire articular surface of the ankle in high-level soccer players.^{7,11,13} The purposes of this study were to identify the distribution of subchondral bone density across the ankle joint surface in 10 asymptomatic soccer players on a highly competitive soccer team and 10 nonathletic volunteers and to assess alterations in the distribution of subchondral bone density associated with soccer activities. Our hypothesis was that soccer activities produce a different pattern of stress distribution in the subchondral bone mineral density of the ankle joint in soccer players compared with controls.

METHODS

Acquisition of CT Image Data

The present study was approved by an institutional review board, and informed consent was obtained from all patients. CT imaging data from both ankles of 10 male volunteers (control group; age 19-25 years, mean age 22.9 years) and 10 male soccer players (soccer group; age 19-27 years, mean age 21.6 years) were collected for further analysis. All participants were volunteers without any ankle symptoms or history of ankle disorders or trauma. The body weight and height were measured. Ankle range of motion was measured using a goniometer. The participants in the control group were volunteers who had not played any sports in daily life since junior high school, and the participants in the soccer group had been on a soccer team since

junior high school. For the soccer group, the mean \pm SD duration on the soccer team was 14.1 \pm 4.2 years.

CT Osteoabsorptiometry

The obtained CT imaging data were transferred to an image analysis system (Revolution CT; GE Healthcare) for further evaluation. A 3-dimensional bone model was created from the transferred axial image data, and then 1 mm-interval sagittal views were reconstructed from the multiplanar reconstruction model. For further evaluation, a customized, originally developed software program was used.¹⁵ On the sagittal images, the region of interest was manually selected so that it included the entire subchondral bone layer of the articular surface of the ankle joint in all slices. After the region of interest was established, x-ray beam attenuation in Hounsfield units (HU; a measurement of density where water = 0 and compact bone = 1000) was automatically measured at each coordinate point at 1-mm intervals. The range of density in each ankle was divided into 3 equal intervals, and the measured densities at each coordinate point were mapped using a 3-grade color scale, with red indicating the highest bone density. The measurement and mapping were repeated in each slice, and by stacking these data, we obtained a 2-dimensional mapping image that projected the distribution of the subchondral bone density.

Quantitative Analysis of the Mapping Images

Quantitative analysis of the mapping images focused on the area and location of higher density areas at each articular surface. The high-density area (HDA) was defined as the upper one-third of the entire range, from the minimum to the maximum HU, in each individual ankle.⁷ The proximal ankle joint surface was divided into 5 parts as follows: anterolateral part of the tibia (AL-Ti), anteromedial part of the tibia (AM-Ti), posterolateral part of the tibia (PL-Ti), posteromedial part of the tibia (PM-Ti), and the fibula. The distal ankle joint surface was divided into the following 4 parts: anterolateral part of the talus (AL-Ta), anteromedial part of the talus (AM-Ta), posterolateral part of the talus (PL-Ta), and posteromedial part of the talus (PM-Ta) (Figure 1A).

The percentage of the HDA (%HDA) at each area of the tibia, fibula, and talus was calculated and compared between the 2 groups. The observer (J.S.) who measured the bone mineral density was blinded regarding the group to which each participant was assigned.

Statistical Analysis

Before analysis, intraobserver reproducibility of CTOAM was calculated on the basis of 5 consecutive measurements, and interobserver reliability was calculated using the measurements of 2 orthopaedic surgeons (J.S., D.M.). The interval between the measurements of %HDA for intraobserver reproducibility was 1 week. The reliabilities between the 2 observers and within each observer were calculated according to the intraobserver, interobserver,

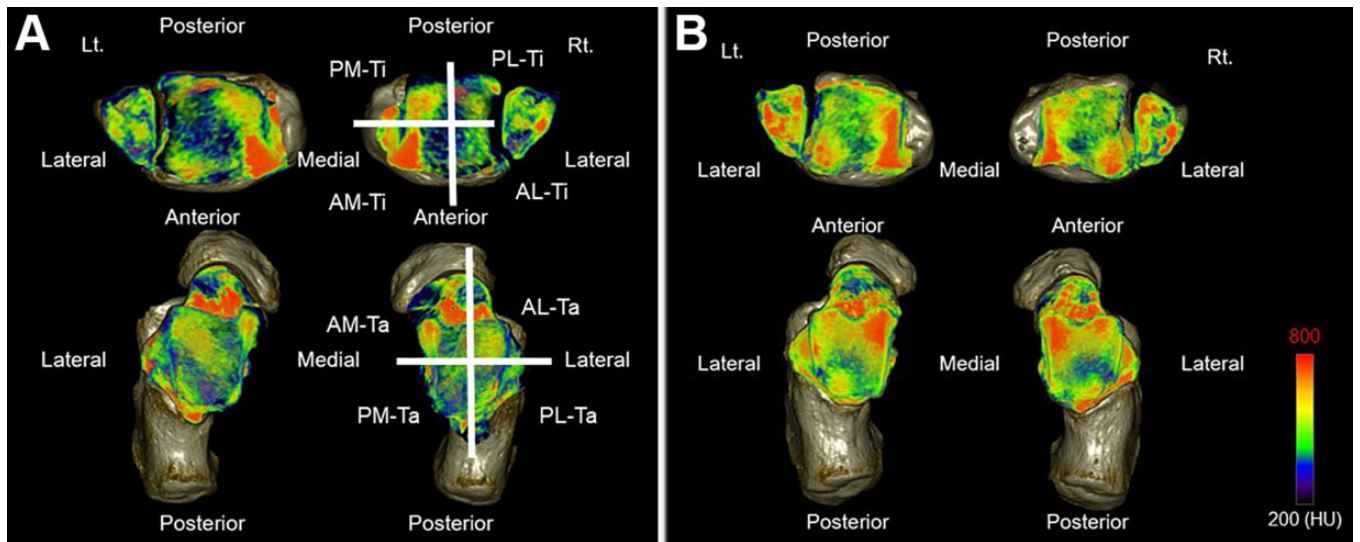


Figure 1. Distribution of subchondral bone density across the articular surfaces of the ankle joint and divided area in the articular surfaces of the ankle joint: (A) control group and (B) soccer group. AL-Ta, anterolateral part of the talus; AL-Ti, anterolateral part of the tibia; AM-Ta, anteromedial part of the talus; AM-Ti, anteromedial part of the tibia; PL-Ta, posterolateral part of the talus; PL-Ti, posterolateral part of the tibia; PM-Ta, posteromedial part of the talus; PM-Ti, posteromedial part of the tibia.

and residual variances estimated by an analysis of variance table that was based on Proc Mixed in SAS software (SAS Institute).

Statistical comparisons of the data of the 2 groups were performed by paired *t* tests, and analysis of variance and the Tukey protected least significant difference test were used for comparisons among >3 areas. Differences were considered significant when *P* values were <.05.

RESULTS

Demographic Characteristics, Intraobserver Reliability, and Interobserver Reproducibility

Demographic characteristics of the participants are shown in Table 1. No significant differences in age, height, weight, or range of motion were found between the 2 groups. The intraclass correlation coefficients for intraobserver reliability and interobserver reproducibility were 0.87 (95% CI, 0.78-0.96) and 0.80 (95% CI, 0.68-0.91), respectively. Drawing on previous results, we considered that the intraobserver and interobserver agreements during CTOAM analysis were acceptable in the current study.

Analysis of the Control Group

In the control group, no apparent difference was seen in the distribution pattern of subchondral bone density between the dominant and nondominant sides (Table 2). The %HDA was greater (*P* < .0001) in the AM-Ti than in other areas (Figure 1A). No other significant differences were found among the areas.

TABLE 1
Characteristics of the Study Group Participants^a

	Control Group (n = 10)	Soccer Group (n = 10)	<i>P</i> Value
Age, y	22.9 ± 2.2	21.6 ± 2.2	.2493
Dominance, n	10 (R) 0 (L)	10 (R) 0 (L)	
Height, cm	170.8 ± 5.9	173.0 ± 5.6	.4013
Weight, kg	58.9 ± 4.4	61.6 ± 4.0	.1689
Range of motion, deg			
Dorsiflexion	9.0 ± 8.8 (R) 11.0 ± 12.0 (L)	15.0 ± 8.5 (R) 14.0 ± 8.4 (L)	.1374 (R) .5253 (L)
Plantarflexion	43.5 ± 22.9 (R) 43.0 ± 24.2 (L)	53.0 ± 10.1 (R) 53.5 ± 10.6 (L)	.2446 (R) .2385 (L)
Eversion	17.0 ± 8.2 (R) 13.0 ± 8.2 (L)	12.5 ± 4.2 (R) 13.5 ± 4.7 (L)	.1419 (R) .8697 (L)
Inversion	29.5 ± 8.3 (R) 28.0 ± 6.7 (L)	33.5 ± 5.8 (R) 30.5 ± 8.3 (L)	.2281 (R) .47 (L)

^aData are presented as mean ± SD unless otherwise noted. L, left; R, right.

Analysis of the Soccer Group

In the soccer group, no apparent difference was seen in the distribution pattern of subchondral bone density between the dominant and nondominant sides (Table 2). The HDAs were predominantly located in the AM-Ti, AL-Ti, AM-Ta, AL-Ta, and fibula (Figure 1B). The %HDA was greater in the AM-Ta than in other areas (*P* < .0001). The %HDAs were greater in the AM-Ti, AL-Ta, and fibula than in the PM-Ti, PL-Ti, PM-Ta, and PL-Ta (*P* < .0001). The %HDA was greater in the AL-Ti than in the PL-Ti, PM-Ta, and PL-Ta (*P* < .0001).

TABLE 2
Comparisons Between the Control and Soccer Groups^a

	Control Group			Soccer Group			P Value, Control vs Soccer	
	D	ND	P Value	D	ND	P Value	D	ND
Tibia								
AM	15.8 ± 4.5	16.0 ± 4.2	.9080	18.7 ± 4.1	19.6 ± 3.9	.6419	.1672	.0770
AL	6.7 ± 2.3	6.2 ± 2.1	.6683	14.4 ± 2.9	14.7 ± 2.6	.8797	<.0001	<.0001
PM	8.2 ± 3.0	8.3 ± 2.5	.9094	10.8 ± 3.4	10.6 ± 2.5	.8940	.0977	.0710
PL	5.5 ± 2.3	5.6 ± 2.1	.9550	6.8 ± 2.4	7.0 ± 1.7	.8407	.2669	.1330
Talus								
AM	7.1 ± 3.6	7.2 ± 2.3	.9556	29.9 ± 5.1	29.7 ± 5.9	.9276	<.0001	<.0001
AL	7.8 ± 2.6	7.2 ± 2.3	.6597	21.2 ± 4.8	21.1 ± 4.8	.9447	<.0001	<.0001
PM	5.4 ± 2.5	5.6 ± 2.3	.8638	5.3 ± 1.8	5.9 ± 2.1	.4878	.9162	.7495
PL	5.9 ± 1.9	6.1 ± 2.2	.8149	5.1 ± 1.7	5.7 ± 2.0	.5238	.3922	.6839
Fibula	6.9 ± 2.5	6.8 ± 2.9	.9508	18.0 ± 5.4	17.4 ± 5.5	.8151	<.0001	<.0001

^aData are expressed as percentage of high-density area (%HDA) and presented as mean ± SD. Boldface indicates statistically significant P values ($P < .05$). AL, anterolateral; AM, anteromedial; D, dominant; ND, nondominant; PL, posterolateral; PM, posteromedial.

Comparisons of %HDA Between the Groups

The %HDA was greater in the soccer group than in the control group. All participants in the soccer group showed HDA widely distributed in the AL-Ti, AM-Ta, AL-Ta, and fibula compared with the control group. The %HDAs in the AL-Ti, AM-Ta, AL-Ta, and fibula were greater in the soccer group than in the control group ($P < .0001$ for all) (Figure 2).

DISCUSSION

We found that the repetitive mechanical stress of soccer activities affected the soccer players' ankle joints. Although several biomechanical studies have reported on the stress distribution in the ankle joint,^{4,9,18} it is difficult to simulate the actual loading conditions of complicated soccer activities by using cadaveric models. To overcome this difficulty, the current study used CTOAM to evaluate differences in stress distributions through the ankle joint in soccer players. This study was novel in that it clarifies the biomechanical characteristics over articular surfaces of the ankle under long-term loading conditions of soccer activities.

The theoretical background of our study methodology is that subchondral bone mineralization adapts functionally to repeated and long-term changes in the load on joints.¹⁷ Therefore, elucidation of the mineralization pattern allows investigators to predict the mechanical condition of the living joints. The present analysis of the ankle joint articular surface demonstrated that HDAs of subchondral bone were located in the anterolateral tibia, anteromedial and anterolateral talus, and fibula in soccer players. The results indicate that repetitive soccer activities distribute excessive stress through these 3 areas in soccer players.

We found that the percentages of HDAs of the ankle joint, including the AL-Ti, AM-Ta, AL-Ta, and fibula, were greater in the asymptomatic soccer players than in the nonathletic volunteers. We also found similar percentages

of HDA distribution around the AM-Ti in both the soccer players and nonathletic volunteers. Calhoun et al,³ using cadaveric ankle joints, demonstrated that as the foot was moved into plantarflexion, dorsiflexion, inversion, or eversion, the total contact area and the average high pressure were altered. The current analysis demonstrated that an HDA of subchondral bone across the articular surface of the ankle joint was located in the AM-Ti in all participants. These results indicate that actual stress across the articular surface of the ankle is located in the AM-Ti in live humans. Additionally, the soccer group showed a significant distribution of the HDA in the AL-Ti, AM-Ta, AL-Ta, and fibula. These different high-density patterns reflect the long-term stress distribution across the ankle joint associated with soccer activities. The cumulative forces of soccer activities thus affect the stress distribution patterns.

Tol et al,²⁰ using mobile sensors and high-speed video, reported that ball impact was predominantly made with the anteromedial aspect of the foot and ankle, with impact between the ball and the base of the first metatarsal bone in 89% of the kicking actions and between the ball and the anterior part of the medial malleolus in 76%. Lees et al¹² reported that the impact force during an instep kick with maximum force, for an ankle velocity of 25 m/s, was approximately 2500 N. These data indicate that the contact between the ball and the medial part of the ankle during kicking motions leads to stress concentration in this part of the ankle. The current analysis demonstrated that an HDA of subchondral bone across the articular surface of the ankle joint in the soccer group was located in the AM-Ta. These findings in the soccer group may stem from the functional adaptation of subchondral bone to the repeated stress across this part of the ankle produced by long-term soccer activities.

Regarding the present study, several considerations must be kept in mind. First, the current analysis was not based on direct measurement of mechanical stress through the ankle joint. The results obtained were relative values rather than

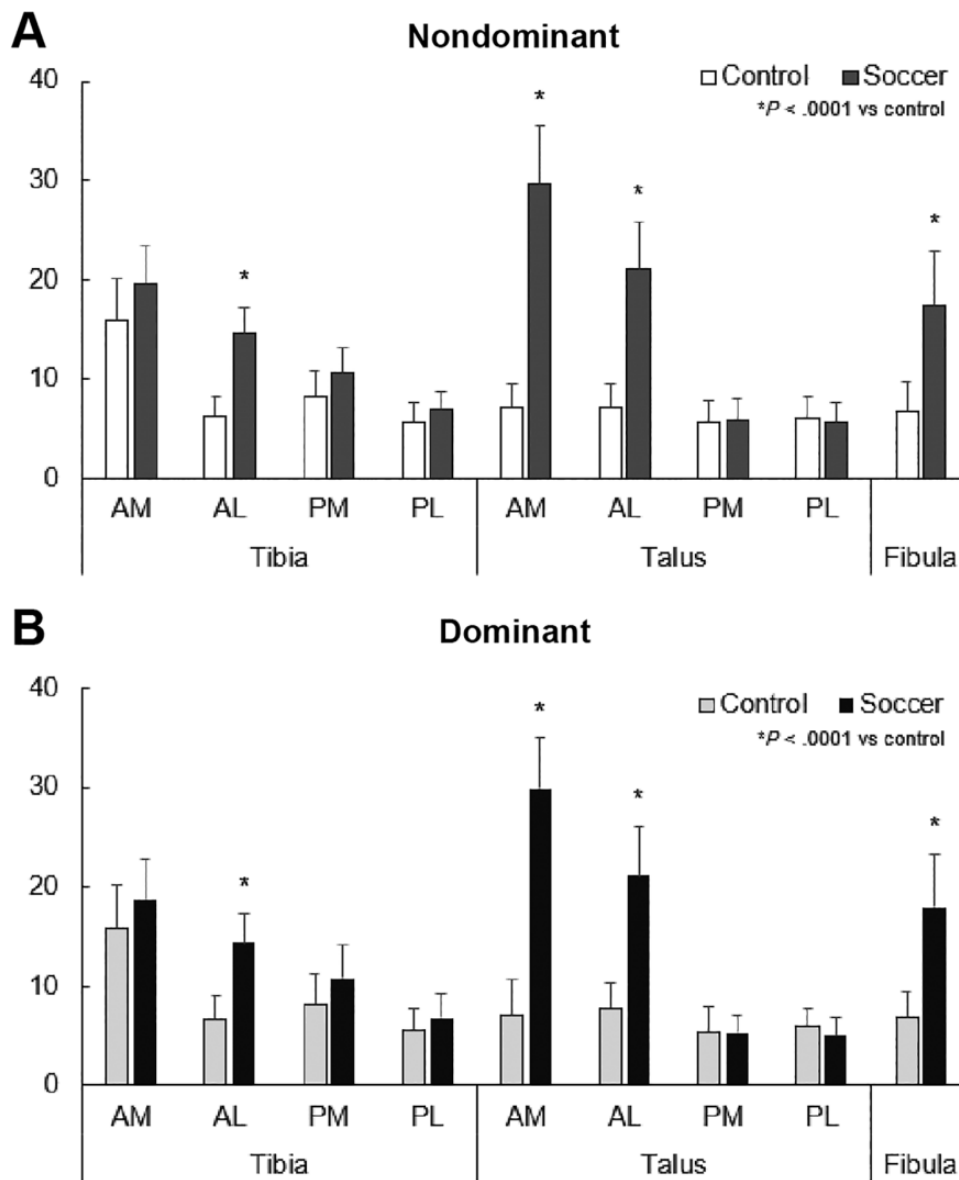


Figure 2. Comparison of the percentage of high-density area between the control and soccer groups for (A) the nondominant side and (B) the dominant side. * $P < .0001$ vs the control group. AL, anterolateral; AM, anteromedial; PL, posterolateral; PM, posteromedial.

absolute values. Second, the pattern of stress distribution through living joints is mainly affected by applied loading conditions and joint geometry. Although the present analysis determined the effects of long-term loading conditions generated by soccer activities on stress distribution through the ankle, the influence of joint geometry was not considered. Further studies will need to be performed to clarify the relationships between the distribution pattern of subchondral bone density and the anatomic parameters of the ankle joints of soccer players. Third, we did not perform an a priori power analysis, and our study may have been underpowered to detect statistical differences. Fourth, the current study was not able to clarify direct relationships between ankle injury and various predictive factors. A

prospective study with a sufficient number of participants will be able to show the relationship between stress patterns and ankle injuries.

In conclusion, the present analysis using CTOAM indicates that the distribution pattern of mechanical stress through the ankle in soccer players is affected by soccer activities.

REFERENCES

1. Brant JA, Johnson B, Brou L, Comstock RD, Vu T. Rates and patterns of lower extremity sports injuries in all gender-comparable US high school sports. *Orthop J Sports Med.* 2019;7(10):2325967119873059.
2. Brockett CL, Chapman GJ. Biomechanics of the ankle. *Orthop Trauma.* 2016;30(3):232-238.

3. Calhoun JH, Li F, Ledbetter BR, Viegas SF. A comprehensive study of pressure distribution in the ankle joint with inversion and eversion. *Foot Ankle Int.* 1994;15(3):125-133.
4. Carson MC, Harrington ME, Thompson N, O'Connor JJ, Theologis TN. Kinematic analysis of a multi-segment foot model for research and clinical applications: a repeatability analysis. *J Biomech.* 2001;34(10):1299-1307.
5. Feria-Arias E, Boukhemis K, Kreulen C, Giza E. Foot and ankle injuries in soccer. *Am J Orthop (Belle Mead NJ).* 2018;47(10).
6. Fousekis K, Tsepis E, Vagenas G. Intrinsic risk factors of noncontact ankle sprains in soccer: a prospective study on 100 professional players. *Am J Sports Med.* 2012;40(8):1842-1850.
7. Funakoshi T, Furushima K, Momma D, et al. Alteration of stress distribution patterns in symptomatic valgus instability of the elbow in baseball players: a computed tomography osteoabsorptiometry study. *Am J Sports Med.* 2016;44(4):989-994.
8. Giza E, Fuller C, Junge A, Dvorak J. Mechanisms of foot and ankle injuries in soccer. *Am J Sports Med.* 2003;31(4):550-554.
9. Goto A, Moritomo H, Itohara T, Watanabe T, Sugamoto K. Three-dimensional in vivo kinematics of the subtalar joint during dorsiplantarflexion and inversion-eversion. *Foot Ankle Int.* 2009;30(5):432-438.
10. Grooms DR, Palmer T, Onate JA, Myer GD, Grindstaff T. Soccer-specific warm-up and lower extremity injury rates in collegiate male soccer players. *J Athl Train.* 2013;48(6):782-789.
11. Irie T, Takahashi D, Asano T, et al. Is there an association between borderline-to-mild dysplasia and hip osteoarthritis? Analysis of CT osteoabsorptiometry. *Clin Orthop Relat Res.* 2018;476(7):1455-1465.
12. Lees A, Asai T, Andersen TB, Nunome H, Sterzing T. The biomechanics of kicking in soccer: a review. *J Sports Sci.* 2010;28(8):805-817.
13. Matsui Y, Funakoshi T, Momma D, et al. Variation in stress distribution patterns across the radial head fovea in osteochondritis dissecans: predictive factors in radiographic findings. *J Shoulder Elbow Surg.* 2018;27(5):923-930.
14. Momma D, Funakoshi T, Endo K, et al. Alteration in stress distribution patterns through the elbow joint in professional and college baseball pitchers: using computed tomography osteoabsorptiometry. *J Orthop Sci.* 2018;23(6):948-952.
15. Momma D, Iwasaki W, Iwasaki N. Long-term stress distribution patterns across the wrist joint in gymnasts assessed by computed tomography osteoabsorptiometry. *J Hand Surg Eur Vol.* 2019;44(10):1098-1100.
16. Momma D, Iwasaki N, Oizumi N, et al. Long-term stress distribution patterns across the elbow joint in baseball players assessed by computed tomography osteoabsorptiometry. *Am J Sports Med.* 2011;39(2):336-341.
17. Muller-Gerbl M, Putz R, Hodapp NH, Schulta E, Wimmer B. Computed tomography-osteabsorptiometry: a method of assessing the mechanical condition of the major joints in a living subject. *Clin Biomech (Bristol, Avon).* 1990;5(4):193-198.
18. Procter P, Paul JP. Ankle joint biomechanics. *J Biomech.* 1982;15(9):627-634.
19. Silva DCF, Santos R, Vilas-Boas JP, et al. Different cleat models do not influence side hop test performance of soccer players with and without chronic ankle instability. *J Hum Kinet.* 2019;70:156-164.
20. Tol JL, Slim E, van Soest AJ, van Dijk CN. The relationship of the kicking action in soccer and anterior ankle impingement syndrome: a biomechanical analysis. *Am J Sports Med.* 2002;30(1):45-50.
21. Walls RJ, Ross KA, Fraser EJ, et al. Football injuries of the ankle: a review of injury mechanisms, diagnosis and management. *World J Orthop.* 2016;7(1):8-19.